Proceedings of the Institute of Acoustics

DIRECT MEASUREMENT OF THE WALL-PRESSURE WAVENUMBER SPECTRUM BENEATH A TURBULENT BOUNDARY LAYER IN A WIND TUNNEL USING A LIMITED NUMBER OF SENSORS.

M. Pognant (1), J.A. Astolfi (2), C. Giangreco (1), B.E. Forestier (2)

(1) Centre d'Etude et de Recherche en Détection Sous-Marine (C.E.R.D.S.M.), DCN Toulon, Chemin de La Gardiole, Le Brusc, 83140 Six-Fours Les Plages - FRANCE.
(2) Institut de Mécanique des Fluides de Marseille (I.M.F.M.), Equipe Aéro-hydrodynamique et Bruit de Champ Proche,1 rue Honorat, 13003 Marseille - FRANCE.

1. INTRODUCTION

This paper presents recent experimental results about the wall-pressure wavenumber-frequency spectrum beneath a Turbulent Boundary Layer (TBL). The actual wavenumber spectrum models are not in agreement especially in the low wavenumber domain. This is a problem because this spectrum component is very important in terms of self noise due to the structural vibration induced by the flow. So, in this paper we test a direct measurement of this excitation with a method of Fourier Transform using limited number of transducers.

Firstly, Discret Fourier Transform estimation (DFT) has been tested on three wavenumber spectrum models (Corcos (1963), Chase (1980), Chase (1987)). Measurement arrays thus constituted are inevitably a limited length which introduces an important bias on the DFT. In order to reduce it, Maximum Likelihood Method (MLM) has been also tried on the same models.

Then, the method was performed on data obtained from a streamwise array of 16 equally spaced transducers flushmounted on a flat plate beneath a turbulent boundary layer. Results are discussed in the last part of this paper.

2. WALL-PRESSURE WAVENUMBER SPECTRUM ESTIMATION.

2.1 Basic principle

The theoretical approach of wave-vector spectrum estimation using a Fourier Transform (DFT or FFT) with an important number of sensors was proposed by Hodgson and Keltie [1] (1984).

N pressure sensors equally spaced at a distance Δx apart, aligned in the streamwise direction on a wall are considered. The outputs of these sensors, $p'_n(x_n,t)$ represent the spatial sampling of the TBL fluctuation pressure field $p'(x,t)$ at the points $x_n=n\Delta x$, $n=0,\dots, N-1$. Time-frequency FFT can be performed on each signal to give N complex frequency vectors $p_n(x_n,\omega)$. To obtain the distribution of energy in the wavenumber domain (k_x,ω), a Fourier Transform in the space domain, is applied. In fact, analogy with time-frequency analysis can be operated : N data points in space will yield N/2 independent wavenumbers :

$$k_m = m\frac{2\pi}{N\Delta x},\ m = 0,\dots, \frac{N}{2}-1 \qquad (1)$$

The highest wavenumber which can be measured correctly by the array is determined by the sensor spacing Δx according to the theorem of Shannon :

$$k_{max} = \frac{\pi}{\Delta x} \qquad (2)$$

k_{max} is the cut-off wavenumber or Nyquist wavenumber. The resolution of filter thus constituted is determined by the length of the array :

$$\Delta k = \frac{2\pi}{N\Delta x} \qquad (3)$$

The main constraint of this method is to choose the spacing Δx between two sensors, so that the total energy contained in the signal be in the analysis range $[-k_{max},+k_{max}]$. Usually, we can consider that the maximum wavenumber of fluctuation pressure field is around $1.5k_{cmax}$ [1], where k_{cmax} is the maximum convective wavenumber which can be determined by ω_{max} and U_c (convection velocity). So, the required sensor spacing is given by :

$$\Delta x = \frac{\pi U_c}{1.5\omega_{max}} \qquad (4)$$

For a wavenumber $k_m = m\frac{2\pi}{N\Delta x}$, the first aliasing lobe occurs at $k'_m = k_m + 2k_{max}$, where the energetic contribution to the wall pressure spectrum is negligible (see figure 1).

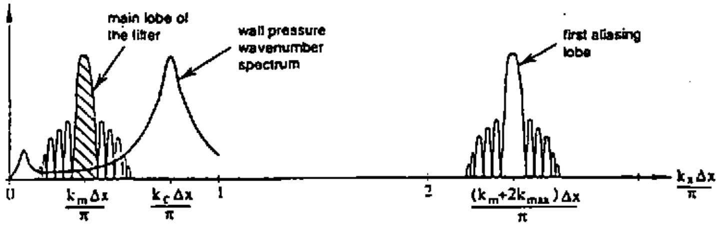

Figure 1 - Transfer function of wavenumber filter based on Spatial Fourier Transform - condition of unaliasing.

Having determined the spacing based on the convective ridge, the wavenumber resolution depends only on sensors number :

$$\Delta k = \frac{3\omega_{max}}{NU_c} \qquad (5)$$

2.2 Practical estimation.

Wakefield and Kaveh [2] (1985) and Tong [3] (1979) describes the methodology to obtain estimator of the wavenumber-frequency spectrum. Firstly, the temporal signal of each sensor is transformed by a FFT algorithm in the frequency domain :

$$p'_m(x_i,\omega) = FFT_t\{p'_m(x_i,t)\} \qquad (6)$$

where $p'_m(x_i,t)$ is the m^{th} temporal record of the signal issued from the i^{th} sensor. Then, the space-frequency cross-spectrum is given by :

$$R_{mij}(\Delta x_{ij},\omega) = p'_m(x_i,\omega).p'^*_m(x_j,\omega) \qquad (7)$$

where $\Delta x_{ij} = (i-j)\Delta x$, represents the spacing between sensors i and j, and "*" denotes the conjugate of a complex number. The final space-frequency cross-spectrum is obtained by averaging of R_{mij} on the M records of the wall pressure field :

$$R(\Delta x_{ij},\omega)=\frac{1}{M}\sum_{m=1}^{M} R_m(\Delta x_{ij},\omega) \qquad (8)$$

Finally, the wall pressure wavenumber can be expressed as follow in matrix notation :

$$F_{1FT} = [e(k_x)]^h R(\omega)[e(k_x)] \qquad (9)$$

where $R(\omega)$ is the Cross-Spectral Density Matrix (CSDM) with NxN elements. The $(i,j)^{th}$ element of the matrix is the value of the cross-spectrum, $R(\Delta x_{ij}, \omega)$ and $e(k_x)$ is the Discrete Fourier vector defined by :

$$e(k_x) = (1, e^{-k_x\Delta x}, e^{-2k_x\Delta x}, \ldots, e^{-(N-1)k_x\Delta x}) \qquad (10)$$

where "h" denotes the conjugate transpose. The finite number of spatial points introduces bias in the DFT. This bias can be reduced using the Maximum Likelihood Method (MLM) which is given by :

$$F_{1MLM}=\frac{1}{[e(k_x)]^h R(\omega)^{-1}[e(k_x)]} \qquad (11)$$

$R(\omega)^{-1}$ is the inverse matrix of $R(\omega)$. MLM reduces the contribution of the wavenumbers which are close to the calculated one.

2.3 Simulations using cross-spectrum models

In order to test these methods on the excitation due to a turbulent boundary layer, three well-known models of wavenumber pressure spectrum were used : Corcos [4] (1963), Chase [5] (1980) and Chase [6] (1987).

An example of the difference between the models is shown in figure 2, where the Corcos and Chase models are compared at1200 Hz and with a free-stream velocity of 10 m/s. The convective ridge is similar and the main difference comes from the spectrum roll-off at the low wavebumbers.

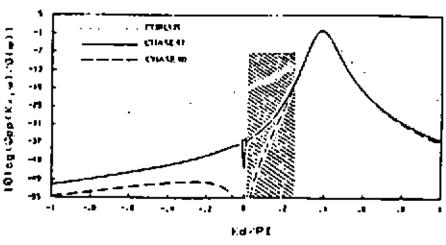

Figure 2 - comparison between Corcos, Chase 80 and Chase 87 models computed at 1200 Hz, with non-dimensional wavenumber kd/π ($d = 10^{-3}$: spacing between sensors, $U_\infty = 10$ m/s, $U_c = 6$ m/s).

The Cross Spectral Density Matrix (used in equations (9) and (11)) was firstly computed by taking an inverse Fourier transform of the wavenumber models, using 512 points. Then the DFT and MLM were performed on the CSDM, with a limited number of spatial points and compared to these models. Figure 3 shows typical results using 16 sensors equally 10^{-3} m spaced, for a free stream velocity of 10 m/s and a convection velocity of 6 m/s at 1200 Hz. The performances of the DFT and the MLM are quite accurate when the Corcos model is used. However, the DFT is unable to follow the spectral roll-off predicted by the Chase models whereas the MLM leads to a good approximation. For instance, around $k_x d/\pi = 0.04$

(vertical dashed line), in the low wavenumber domain, the difference between the model and the DFT is 25 dB against 5 dB with the MLM.

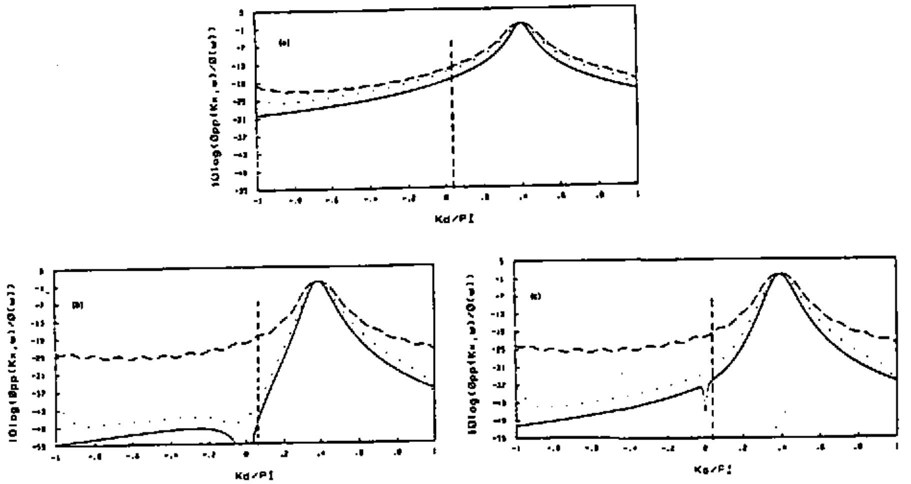

Figure 3 - Comparison between computed analytical Corcos (a), Chase 80 (b) and Chase 87 (c) models and estimations. - - - - - - - DFT · · · · · · · · · · MLM ———————— analytical model.

The basic DFT filter shape for the uniform window function presents a difference of 13 dB between the main lobe and the highest side-lobe which is of the same order than the value proposed by Corcos model between the convective ridge and the low wavenumber domain level. This explains the good results obtained with the DFT estimation on the Corcos model. As far as Chase models are concerned, the decrease of the spectrum below the convective ridge is too important compared to the side-lobe leakage of the DFT computed with 16 points. Nevertheless, the MLM estimation follows the two models proposed by Chase and therefore seems to reduce the bias due to the small length of the array.

The main parameter of the array is the number of sensors. In figure 4, the difference between the estimation and Chase model (1987), at $kd/\pi = 0.04$, is plotted. As known, the increase of the sensor number leads to a better estimation of the wall pressure spectrum. Furthermore, the length of the array has to be less than the streamwise correlation length of the wall-pressure field. However, the MLM method leads to less accurate results when the number of sensors is too important.

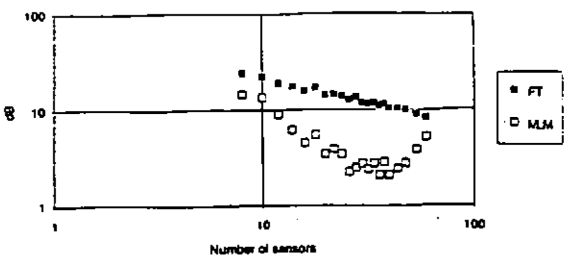

Figure 4 - effect of the sensors number on the estimations for the Chase 87 model at $kd/\pi = 0.04$ and 1200 Hz.

As majority of authors generally consider Chase model better than Corcos model especially in the low wave number domain, it can be considered, according to this results that the DFT could be inadequate to estimate the wavenumber spectrum in this region. Nevertheless, the DFT and the MLM has been performed on experimental data.

3. EXPERIMENT SET-UP AND RESULTS

The experiments was carried out in the wind tunnel of Fluid Mechanics Institute in Marseille. A turbulent boundary layer was developed along a flat plate. The characteristics of the TBL obtained from hot-wire measurements are given on Table 1.

X (m)	U_∞(m/s)	δ (mm)	δ_1 (mm)	θ (mm)	H	τ_p	U_τ (m/s)	$10^3 C_f$	$R_{e\tau}$	$10^{-6} R_{ex}$
3,4	12	64,8	8,37	6,27	1,33	0,27	0,46	3,03	2.1 10^4	2,81

Table 1 - main characteristics of the TBL.

16 transducers were used to measure the wall-pressure fluctuations. The transducer and array characteristics are given on Table 2.

Array	Number	16
	Δx (mm)	3.5
	Total length (mm)	56
	k_{max} (m^{-1}) (unaliased region)	898
	Δk (m^{-1}) (resolution)	112
Sensors	Type	piezoelectric transducer
	Constructor	Endevco (USA)
	Model	8507-2 (2 PSI)
	Outer diameter (mm)	2.6
	Sensitivity	25 µV/Pa

Table 2 - array and transducers characteristics.

The calibration of each transducer was obtained by measuring the response to a calibrated acoustic excitation (B&K 4230 Source delivering -94 db ref 20 µPa at 1000 Hz). The gain of each transducers was adjusted in sorder to obtain the same response to the same excitation. Furthermore, the linearity of the magnitude and phase response were measured at the CERDSM.

Then, in wind tunnel using this array, 32 blocs of 1024 temporal points were recorded for each sensors with a 20Khz sampling frequency. Figure 5 shows the isovalues of the wall-pressure spectrum computed from the DFT, versus the frequency and the non-dimensional wavenumber $k_x d/\pi$.

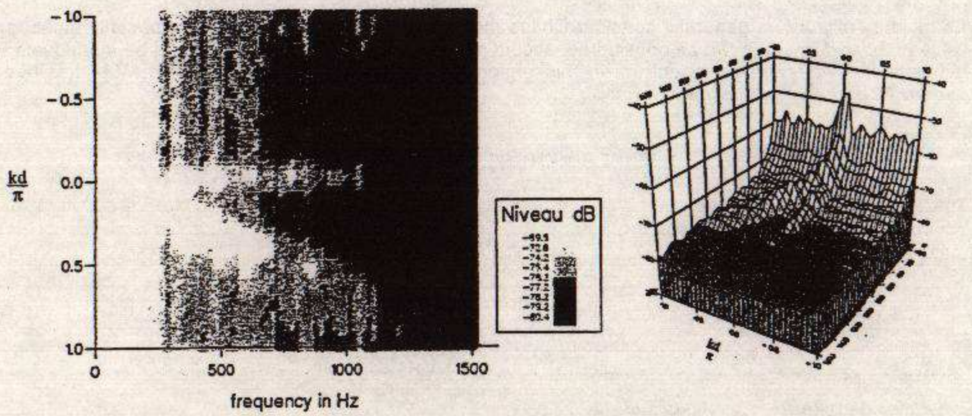

Figure 5 - Normalised spectrum $F1(\frac{k_x d}{\pi}, o, \omega)$ measured at 12 m/s, DFT estimation.

It's interesting to note that the well-known shape of the TBL pressure field can be obtained directly with an array of 16 sensors. Indeed, the convective ridge at $k_x=\omega/U_c$ and the acoustic peak centred on $k_x=\omega/c_o$ (c_o : sound celerity in air) can be clearly observed. Cuts at a fixed frequency (from 200 Hz to 1200 Hz) are shown in figure 6 and 7.

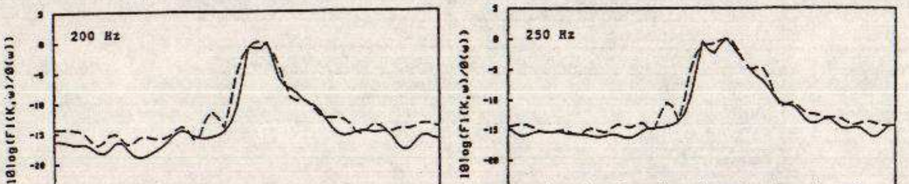

Figure 6 - Normalised spectrum $F1(\frac{k_x d}{\pi}, o, \omega)$ measured at 12 m/s for various frequencies. ---- DFT ——— MLM.

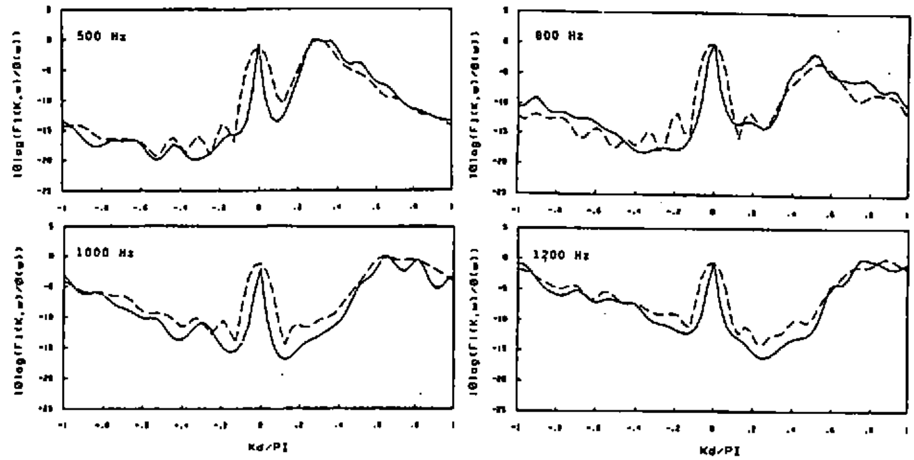

Figure 7 - Normalised spectrum $F1(\frac{k_x d}{\pi}, 0, \omega)$ measured at 12 m/s for various frequencies. - - - - DFT ———— MLM.

It is observed, a wide peak on the right side corresponding to the convective ridge and an other peak centred around $k_x=0$, corresponding to the acoustic contribution which comes from the background noise of the wind tunnel. At low frequencies, the two peaks are very close and tend to disjoint as the frequency increases. The MLM allows to differentiate the convective ridge and the acoustic peak as early as 200 Hz. These results are in agreement with those of Sherman [7] (1990). Nevertheless, the amplitude of low wavenumber is found to be 15 dB down the convective ridge compared to 28 dB found by Sherman or 22 dB found by Manoha [8] (1991). In fact, the background noise of the facility introduces an acoustical singularity (not due to the TBL) which can disturb the estimations. In order to take into account of this external contribution, the background noise was simulated, adding on Chase 87 model, an arbitrary level peak centred around the acoustic number (figure 8).

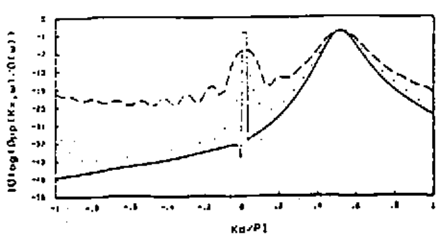

Figure 8 - effects of external acoustic disturbance on the chase 87 model. - - - - - - - DFT · · · · · · · · · · MLM ———————— analytical model.

In fact, the external acoustic contribution is seen as a plane acoustic wave propagating in the streamwise direction. The figure 8 shows clearly that the acoustic perturbation increases the estimated low wavenumber spectral level and that the estimations have difficulties, in that case, to follow the modified wall-pressure model.

4. CONCLUSION

i) This study shows that the turbulent boundary layer wall-pressure wavenumber spectrum can be measured using a spatial Fourier Transform with a limited number of transducers.

ii) The global shape of the TBL pressure field over a large wavenumber domain can be directly obtained with an array of 16 sensors (from the acoustic wavenumber up to the convective ridge).

iii) It has been shown that the background noise can disturb the spectrum estimation at low wave numbers.

News experiments are in progress in order to complete the present experimental results. Following subject are checking : increasing of the spatial pressure resolution using pin-hole transducers, improving the frequency resolution and attenuating the background noise of facility.

5. REFERENCES

[1] T.H. HODGSON, R.F. KELTIE, 'An innovative fast Fourier transform array technique for low wavenumber measurements of the turbulent boundary layer fluctuating pressure field', Symposium on Flow-Induced Vibrations, ASME WAM, Vol. 5, pp. 39-51, 1984.
[2] G. H. WAKEFIELD, M. KAVEH, 'Frequency-wavenumber spectral estimation of the wall-pressure field beneath a turbulent boundary layer', ASME, Shear Flow-Structure interaction phenomena, A. Akay & M. Reischman Eds., 1985.
[3] P.S. TONG, F.L. REES, 'TBL wavenumber Spectral measurement using Maximum Likelihood Methods', Binary System Inc., ONR Contract No. N00014-72-C-0318, 1979.
[4] G.M. CORCOS, 'The resolution of pressure in turbulence', Journal of Acoustical Society of America', Vol. 35, pp. 192-199, 1963.
[5] D.M. CHASE, 'Modeling the wavevector-frequency spectrum of turbulent boundary layer wall pressure', J. Sound Vib.,Vol. 70(1), pp. 29-67, 1980.
[6] D.M. CHASE, 'The character of the turbulent wall pressure spectrum at subconvective wavenumbers and a suggested comprehensive model', J. Sound Vib.,Vol. 112(2), pp. 125-147, 1987.
[7] C.H. SHERMAN, S.H. KO, and B.G. BUEHLER, 'Measurement of the turbulent boundary layer wave-vector spectrum', Journal of Acoustical Society of America', Vol. 88, pp. 386-390, 1990.
[8] E. MANOHA ,'Wall pressure wavenumber-frequency spectrum beneath a turbulent boundary layer measured with transducer arrays calibrated with an acoustical method', ASME Winter Annual Meeting, Atlanta, GA (USA), 1991.